

# Surface Roughness Prediction of EN8 components using deep learning neural network

Ghanshyam Patel<sup>a</sup> and M.B.Kiran<sup>a</sup>

<sup>a</sup>Department of Mechanical Engineering,School of Technology,Pandit Deendayal Energy University

## ABSTRACT

EN8 is widely used in die making industry. The Dies made by Electric Discharge Machining process function properly only when it has the required surface finish. Thus surface roughness measurement helps in assessing the functioning of the die when it is put in to service. Many of the previously developed ANN models used to predict only Average roughness  $R_a$ . For proper assessment of Die performance other roughness parameters such as  $R_q$ ,  $R_z$ ,  $R_v$  and  $R_p$  are also required. In this context the present surface roughness prediction model using ANN assume special significance. The results obtained from ANN model are validated by comparing with the results of RSM prediction model. Network trained with LM algorithm is found to be the best ANN model to predict surface roughness parameters such as,  $R_a$ ,  $R_q$  and  $R_v$  and GD algorithm is best for  $R_z$  and  $R_p$ . Using separate testing set, the network is also tested and it is observed that the experimental and predicted values are in proximity to each other.

## KEYWORDS

Roughness measurement, Response surface method (RSM), Electrical discharge machining (EDM), Roughness prediction, Artificial neural network (ANN)

## 1. Introduction

Surface roughness is a significant parameter of any machined component. By knowing the surface roughness, it is possible to determine the suitability of the component when it is put into service. Thus, it can be considered an index of the quality of the product. Many aerospace components such as engine piston heads, landing gear etc., are being manufactured by EDM. It is popular because the desired surface finish can be achieved easily, even with hard-to-machine materials. In this machining process, copper or any conductive metal electrode is used as the negative terminal, and the component to be machined is connected to the positive terminal. A very high temperature generates enough spark for enough heat to erode the workpiece component. The dielectric liquid will constantly flush out tiny particles from the machined surface to cool metal pieces and electrodes. It also controls the temperature so that the surface is not damaged. Surface roughness is a vital parameter in all industrial applications including Die making. Since Artificial intelligence's(AI) invention, many researchers have been applying it to many fields, including die making. A popular method for extracting information from unstructured data is the artificial neural network. The extensive connectivity of neurons used in model-based ANN design enhances performance. The input, hidden, and output layers are used by the algorithm presented in this paper.

This algorithm determines an initial set of weights and specifies how weights will be applied to improve performance during the training phase. A neuron's reaction to a signal it receives is controlled by an activation function. The sigmoid function is the most frequently utilized. The objective of the current research work is to develop an AI based model to predict surface roughness parameters- $R_a$ ,  $R_q$ ,  $R_z$ ,  $R_p$ ,  $R_v$ . Earlier attempts by researchers included only prediction of  $R_a$  as roughness parameter. Complete characterization of dies require  $R_q$ ,  $R_z$ ,  $R_p$ ,  $R_v$  parameters (Table1) as well. In this context the current research work assumes special significance.

### 1.1. The surface roughness parameters examined

#### Surface Roughness Parameters

##### (1) Arithmetic average height ( $R_a$ )

This is one of the best-known surface roughness parameters figure 1 . It is the most often used characteristic in the industry because it is easy to measure and define.

$$R_a = \frac{1}{L} \int_0^L |y(x)| dx \quad (1)$$

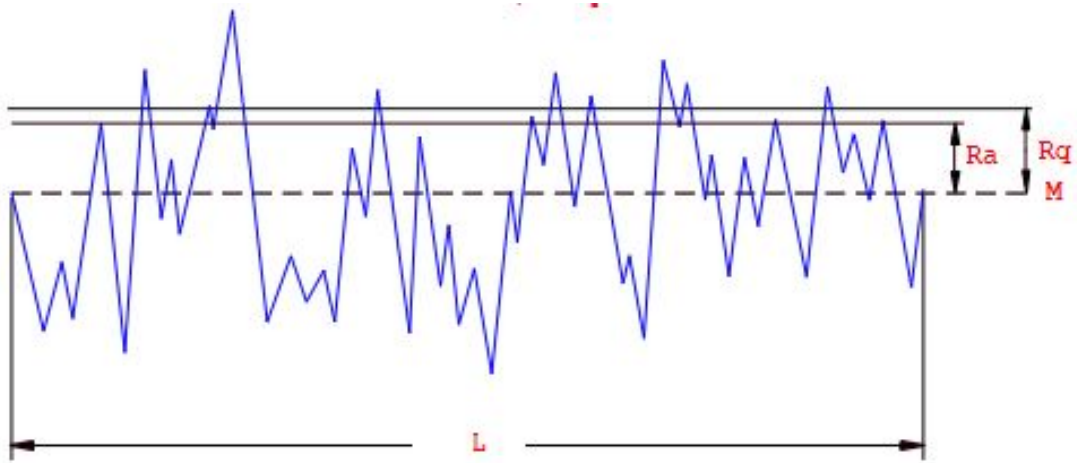


Figure 1.: Arithmetic average height ( $R_a$ ) and Root mean square ( $R_q$ )

- (2) **Root mean square roughness ( $R_q$ )**  $R_q$  represents the standard deviation of the distribution of surface heights, so it is an important parameter to describe surface roughness with statistical methods. This parameter is more sensitive to large deviations from the mean line than the arithmetic average height ( $R_a$ ) as shown in fig. 1

$$R_q = \sqrt{\frac{1}{L} \int_0^L y(x)^2 dx} \quad (2)$$

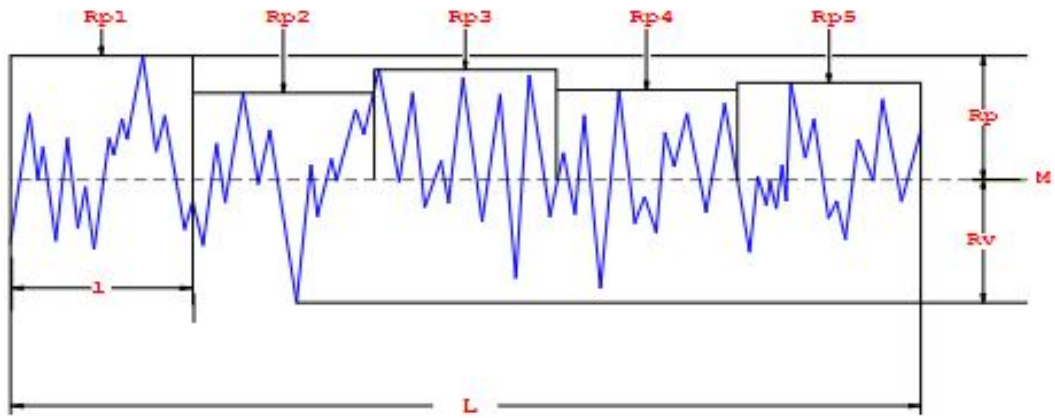


Figure 2.: Represents the  $R_z$ ,  $R_p$  and  $R_v$  parameter,

### (3) Ten-point height ( $R_z$ )

The ten-point height is more sensitive to extreme values (valleys, peaks) than  $R_a$ . The international ISO system defines this parameter as the difference in height between the average of the five highest peaks and the five lowest valleys along the assessment length of the profile as shown in fig. 3

$$R_z = \frac{1}{n} \left( \sum_{i=1}^n P^i + \sum_{j=1}^n V^j \right) \quad (3)$$

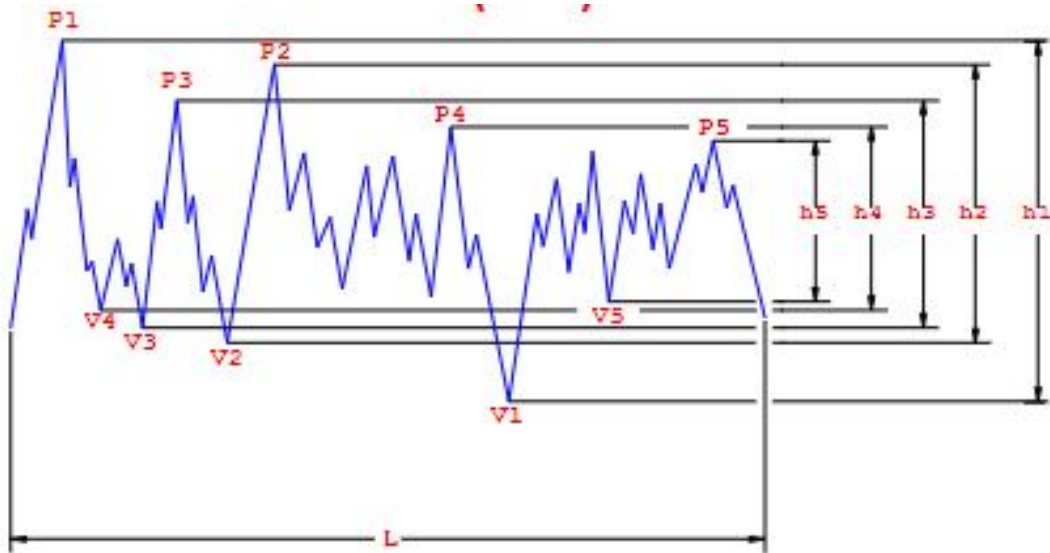


Figure 3.: The ten-point height ( $R_z$ )

### (4) Maximum height of peaks ( $R_p$ ) $R_p$ is defined as the maximum height of the

profile above the mean line within the assessment length as in Fig. 4.

$$R_p = \max(Rp^i) \quad (4)$$

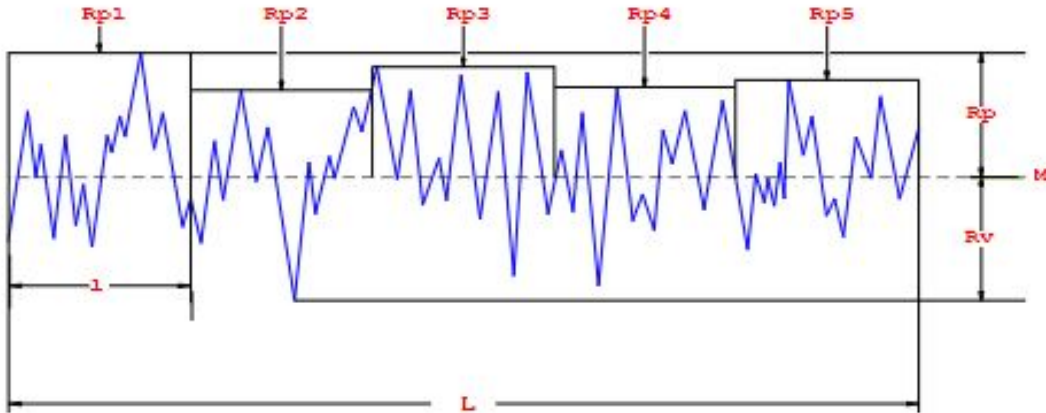


Figure 4.: Maximum height of peaks ( $R_p$ )  
and maximum depth of valley ( $R_v$ )

- (5) **Maximum depth of valleys ( $R_v$ )**  $R_v$  is defined as the maximum depth of the profile below the mean line within the assessment length as shown fig. 4

$$R_v = \max(Rv^j) \quad (5)$$

Table 1.: Types of Surface Roughness Parameters and its Industrial Applications

Roughness	Full Name	Industrial Applications
Ra	Arithmetic Average Roughness	Quality control in manufacturing, functional performance of components, aesthetics in consumer products.
Rq	Root Mean Square Roughness	Tribology studies, friction and wear resistance optimization, surface coating applications.
Rz	Maximum Height of the Profile	Functional performance in sealing surfaces, tribology studies, adhesion in surface coatings.
Rp	Maximum Peak Height	Friction and wear resistance optimization, adhesive bonding in assembly processes.
Rv	Maximum Valley Depth	Friction and wear resistance optimization, adhesive bonding in assembly processes.

## 2. Literature survey

Anurag et al. studied surface roughness of EN-8 tool steel workpiece in the die sinking EDM machine. Surface roughness was measured and analyzed. Effects of machining parameters viz. discharge current, T-ON pulse on time, T-off pulse off time, wire feed, servo voltage, MRR and surface roughness were observed and concluded that for more time taken for machining then low MRR and more Rz value and for less time taken for machining, less Rz value. [1].

Gyuweon Jung, et al. The principal component analysis (PCA) and deep neural network (DNN) are used to classify the gas types. The (100-MAPE) versus epoch for different preprocessing methods are shown using figures. Using more than 20 and 10 neurons in the two hidden layers, DNN has successfully demonstrated accurate identification of gas concentrations.

Madhumitha Ramchandran et al. developed a neural network model capable of predicting the margin to the boiling crisis (i.e., the departure from nucleate boiling ratio, DNBR). They used a feature ranking algorithm and the trained neural network model was used to determine the DNBR with a mean absolute percentage error complement (i.e., 100-MAPE) of 96% [2].

Mustafaiz et al. investigate L18 Orthogonal Array (OA) tests were conducted using input factors such as Peak Current, Duty Cycle, and Voltage Gap. Studies were conducted to determine how machining parameters impacted responses like MRR [3].

Ushasta Aich et al. In this study, support vector machines, and PSO are employed to create EDM modeling frameworks. Models for MRR and Ra are created using SVM. To confirm the models' correctness and applicability, testing data sets are used to evaluate them [4].

Balsubramaniam et al. focus the major focus of this study is wire electric discharge machining (W-EDM), which is used in SMA. When analyzing machining parameters, such as surface and material removal, current, servo voltage, and pulse on time were taken into account. Pulse-free time. Parametric analysis was completed after the response surface approach-based central composite design [5].

The author investigate an ANN model has been created by the authors to forecast the surface roughness of EN 31 steel. Average roughness (Ra) is the output neuron, whereas machining parameters are the input neurons. A CCD serves to conduct experiments. Based on performance indicators, the best network is chosen after comparing several training techniques. Results from the L-M algorithm are good. When predicting surface roughness, the ANN model outperforms the RSM model. To examine how process variables affect results, 3D surface plots are employed [6].

Allesandro Giusti et al. investigate a Convolutional Neural Network is employed in a cheap optical measurement system that is combined with an EDM machine to forecast Ra values. Experimental results show that predictions made at different roughness levels are accurate. This is an effective method for characterizing and controlling the roughness of surfaces in machining operations [7].

Ashish Goyal et al. use surface roughness optimization on an EDM machine. The Taguchi approach has optimized the results that were achieved. ANOVA analysis reveals important criteria for enhancing surface roughness [8].

Naresh et al. focus on Levenberg-Marquardt (LM) algorithms. It was discovered that LM with 10 neurons was the ideal algorithm and number of neurons in the hidden layer for ANN models [9].

Je-Kang Park et al. focus on artificial intelligence (AI) and smart sensors to automatically detect surface flaws in components. The suggested technique uses CNN-based

image processing to find wear, scratches, and burrs. The efficiency of a single CNN network for assessing various sorts of flaws on textured and non-textured surfaces was demonstrated through the construction and testing of several neural networks [10].

R.K.Patel et al; focus on Sorface roughness and EDM machining parameters Ton, Vgap, Duty cycle. Using Response surface Method Ton is found o be dominant parameters[11] .

Dhiren Patel et al. focus on machine learning and image processing techniques are used to identify surface quality from machining surfaces. It offers a technique that uses machine learning algorithms to characterize collected photos by extracting statistical information from them. Results with the ANN and RF algorithms demonstrate remarkable accuracy. This study provides a practical method for evaluating machined surfaces' quality, which is advantageous to sectors including manufacturing and quality control [12].

Uma Maheswari,Reddy Patauri et al. Surface roughness significantly improves by 61.31 when the GA technique is used. These outcomes represent quick and precise WEDM of Inconel 718 prediction and optimization approaches [13].

T. R. Paul et al. investigate the optimization process parameters in Inconel 800 EDM using a hybrid approach. It is very simple to use MOORA, or multi-objective optimization on the basis of ratio analysis, and it is also very simple mathematically.[14].

Routara et al. focus on the EDM machining properties of T6-Al7075. For both rotary and steady tool modes, the parameters Tonne, Toff, Ip, and voltage are used. MRR TWR, Ra, and Rq optimization for responses has been examined [15].

Jamal Seedi et al. investigate the research describes the use of deep neural networks in an industrial measurement system for determining surface roughness and fault detection on degraded steelwork parts. The suggested techniques are superior to others. By combining CNN-based regression with CNN-based classification, we achieve accurate roughness estimation (7.32% error), high defect detection accuracy (97.26%), and precise localization (99.09% area under the ROC curve)[16].

Shivanna et al use this study compares 3D surface roughness metrics using a confocal and CCD camera using aluminum as a specimen metal. The vision approach is a revolutionary technique. [17]. Ranjit Singh et al In this study, EDM settings for a Cu-based shape memory alloy are optimized using machine learning techniques. The study examines how dimensional deviation and tool wear rate are affected by process parameters. The study makes use of a central composite design matrix and employs 2-D and 3-D graphs to illustrate response parameter behavior. Cu-based SMA machining in EDM processes and optimization by Genetic Algorithm, and Teacher Learning-based optimization approaches both involve machine learning [18].

Mustafa Ulas et al.focus on Aluminum alloys are precisely machined using WEDM and can estimate surface roughness, saving time and money compared to experimentation. Al7075 aluminum alloy experiments were conducted with various WEDM parameters, and machine-learning models for surface roughness prediction were built. The model has the accuracy of 0.9720 and has the most potential for use in manufacturing WEDM-produced parts [19] .

Vinay Vakharia et al. focus on Nitinol in manufacturing for biomedical and aeronautical applications is examined in this research. The difficulty of producing desired surface characteristics in machined components is discussed in the paper. FESEM (Electro Microscope) is utilized to analyze the surfaces of Nitinol specimens after wiring electrical discharge machining. Surface morphology and its link to process parameters are predicted using deep learning models, such as SinGAN and DenseNet.

A useful tool for surface image prediction in manufacturing, the DenseNet model has great accuracy [20].

Hatice Varol et al use the metal alloy Inconel 718 have excellent mechanical, corrosion-resistance, and high-temperature performance characteristics. However, problems arise from their low machinability and the necessity for expensive tools in conventional machining techniques. For cutting hard materials, non-traditional production techniques like electrical discharge machining offer an affordable solution. An artificial intelligence model for evaluating surface roughness based on process parameters was developed using ANN and GEP[21]. Yogesh et al. draw attention to the difficulties in determining the ideal parameters for the highest MRR and the lowest Ra as well as the limitations of conventional testing techniques. The suggested approach uses Decision Tree and Naive Bayes algorithms to forecast SR and MRR, saving time and important resources. The emphasis is especially on the EDM machining of aluminum composites, demonstrating how the algorithms can be used in this situation[22].

Zhang et al. focus on .selective laser melting (SLM) used back propagation neural networks (BPNN)which quickly predict the surface roughness with high prediction accuracy [23].

Kundrak et al. focus on surface roughness of machined hard material with Ra,Rq,Rz,Rsk,Rku parameter textbf [24].

Ilah Asilruk et al. proposes surface roughness model for turning process.comparision of ANOVA and ANN results indicates that ANN predicts more accurately for turning process[25]

### 3. Methodology

#### 3.1. Specimen preparation

Generally, for three parameters and at three levels need 27 ( $4^3$ ) numbers of experiments to be conducted. Central composite design of experiment suggests very less number of experiments to predict optimized conditions among the assigned parameters with their levels. Taguchi L27 array is found to be suitable for this experimental approach of study. Hence, only 27 experiments are required to be conducted to find the combination of levels of parameters, which give the optimal result. Analysis of Variance (ANOVA) is performed to observe the effects of process parameters. By altering settings during an EDM machining operation, specimens are prepared. In Table 2,  $I_p$ ,  $T_{on}$ ,  $T_{off}$  are variables and peak Voltage is kept constant When performing an EDM operation on specimens, die electric fluid is employed.

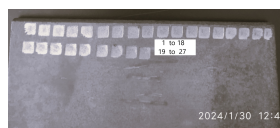


Figure 5.: EDM 27 Nos.specimens on EN8 plate



Figure 6.: EDM machine - Sparkonix

Table 2.: Input parameters

Design factors	Code	Levels		
		-1	0	1
Pulse on time(Ton)µs	A	3	5	7
Pulse off time(Toff)µs	B	2	4	6
Discharge Current(Ip)amp	C	10	20	30

### *3.2. surface roughness measurement*

Surface roughness of the specimens, made with different process parameters, are measured (Table 3) using a profilometer of Mitsubishi model SJ-410 as shown in Figure 7 sets of observations are obtained and the average values are computed for Ra, Rq, Rz, Rp, Rv



Figure 7.: Profilometer-SJ410

Table 3.: Process parameters and Roughness details of Specimens

No	Ton	Toff	Ip	Ra	Rq	Rz	Rp	Rv
1	3	2	10	4.252	5.585	28.935	12.071	16.865
2	3	2	20	4.442	5.664	26.886	10.423	16.462
3	3	2	30	5.428	6.928	29.213	14.856	14.356
4	3	4	10	4.317	5.309	24.604	10.612	13.992
5	3	4	20	4.489	5.518	25.57	10.429	14.141
6	3	4	30	5.061	6.529	29.292	13.338	15.954
7	3	6	10	4.047	5.047	23.099	9.117	13.982
8	3	6	20	4.372	5.399	23.959	12.019	11.94
9	3	6	30	4.681	5.705	23.789	10.131	13.658
10	5	2	10	4.296	5.735	27.909	14.507	13.402
11	5	2	20	4.706	6.136	27.858	11.558	16.3
12	5	2	30	5.077	6.45	29.005	12.618	16.388
13	5	4	10	4.506	5.695	25.707	9.887	15.82
14	5	4	20	4.761	5.803	25.066	10.824	14.242
15	5	4	30	5.561	6.807	28.956	13.056	15.9
16	5	6	10	4.742	5.915	26.665	12.601	14.064
17	5	6	20	4.864	6.344	27.857	11.205	16.651
18	5	6	30	6.48	8.296	35.502	18.892	16.61
19	7	2	10	3.936	4.971	22.736	9.606	13.13
20	7	2	20	4.278	5.611	27.583	15.535	12.048
21	7	2	30	5.007	6.013	25.309	11.77	13.539
22	7	4	10	4.133	5.202	24.117	11.084	13.033
23	7	4	20	4.389	5.409	24.965	10.593	14.372
24	7	4	30	5.177	6.337	26.83	10.833	15.997
25	7	6	10	4.746	5.719	25.865	10.565	15.3
26	7	6	20	5.016	6.19	27.16	11.631	15.53
27	7	6	30	5.274	6.357	27.608	11.603	16.004

### 3.3. Development of model using Artificial Neural Network (ANN)

A neural network is made up of a number of layers that each contain various components known as neurons. Network formation determines the network's type. Weights are used in the learning process to convert the network's storage of processing power. The training algorithm is a process that involves changing a network's weights to reduce a chosen function of error between the actual and desired outputs [1]. Today's industrial applications use ANN. ANN can be used in a variety of manufacturing processes. Input, hidden, and output layers make up its three primary layers. The input layer's neurons send information from the outside environment to the hidden layer. Utilizing data from the input layer and the activation, bias, and summation functions, outputs are generated in the hidden layer. The ANN's workings are displayed in Figure 8. The model is developed using Leven Berge-Marqardt algorithm with Adam optimizer. Convolutional Neural Networks (CNNs) are being trained by the authors to analyze and characterize the topology of a surface using the current methodology. The objective is to develop a method that can accurately assess surface topology using CNNs. This machine can generate surfaces with standard characteristics, which are essential for training the CNN models. By producing surfaces with

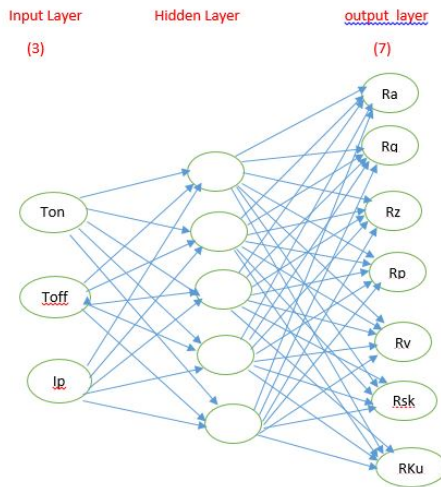


Figure 8.: Neural Network

known characteristics, they can train the CNNs to accurately identify and characterize different surface topologies. The researchers aim to create a robust and versatile system that can analyze and classify surfaces based on their topology, regardless of the specific roughness average (Ra) value. This work has the potential to enhance the understanding and characterization of surfaces in various industries and applications[2]. In the era of rapid development of science and technology, people's requirements for intelligence are getting higher and higher, and artificial intelligence has set off a new wave. Artificial neural networks (ANN) is a computational model that mimics biological neural networks. It evolved from the single-layer perceptron M-P model proposed in 1943 to a computing model that now has a multilayer perceptron network.<sup>13–16</sup> The computational power is greatly improved and can deal with complex nonlinear problems. It is widely used in model recognition, machine vision, speech recognition, and other artificial intelligence fields. A BP neural network is a feed-forward artificial neural network using an error back propagation algorithm, it has strong adaptive

self-learning ability, superior fault tolerance, and robustness, and is the most widely used of the neural network models. BP neural networks structure is divided into three layers, namely, the input layer, hidden layer, and output layer, through the connection between each layer connection weights and threshold values, as shown in Figure 1. The basic principle is that the input vector flows through the hidden layer and the output layer of the inter-layer transfer function. If the demand is not met, the output value of the neuron is returned. The learning process is modified by modifying the connection weight and threshold value. The whole process continues until the output value meets the requirements and terminates.[23]

The following metrics, defined by equations 1,2 and 3, will be used for testing the efficacy of the prediction model.

Mean Squared Error (MSE):

$$\text{MSE} = \frac{1}{N} \sum_i |t_i - o_i|^2 \quad (6)$$

Mean Absolute Percentage Error (MAPE):

$$\text{MAPE} = \frac{1}{N} \sum_i \left| \frac{t_i - o_i}{t_i} \right| \times 100 \quad (7)$$

R-squared ( $R^2$ ):

$$R^2 = 1 - \frac{\sum_i (t_i - o_i)^2}{\sum_i (o_i)^2} \quad (8)$$

### CNN model summary :

- neworkt = feedforwardnet
- architecture :
  - Input layer = 1 with 3 neurons
  - Hidden layer = 8 with 3 to 10 neurons each
  - output layer = 1 with 5 neurons
- No. of Optimizers = 4
  - Names of optimizers =traingd, traingda , trainlm, trainrp
- divide function = 'dividerand';
- TrainRatio = 0.7;
- Validation Ratio = 0.15;
- Test Ratio = 0.15;
- No. of epochs = 10;
- Learning rate = 0.01;

### 3.4. Prediction using Response Surface Method(RSM)

Multiple regression is statistical technique to determine predicted values. In order to predict roughness parameters  $R_a$ ,  $R_q$ ,  $R_z$ ,  $R_p$ ,  $R_v$  Equation 9 is used.

$$Y = \beta_0 + \sum_{i=1}^k \beta_i \cdot X_i + \sum_{i=1}^k \beta_{ii} \cdot X_i^2 + \sum_{j>1}^k \beta_{ij} \cdot X_i \cdot X_j + \varepsilon \quad (9)$$

where Y represents the corresponding response, i.e.,  $R_a$  of EDM process in the present work,  $X_i$  is the input variables,  $X_i^2$  and  $X_i \cdot X_j$  are the squares and interaction terms, respectively, The influences of EDM parameters ( $T_{on}$ ,  $T_{off}$ ,  $I_p$ ) on surface roughness ( $R_a$ ) have been assessed for EN8 steel. The second-order model is the relationship between the surface roughness parameter and the Multiple regression is a statistical technique that allows us to determine the correlation between a continuous dependent variable and two or more continuous or discrete independent variables.

Results obtained by using RSM model will be elaborated in section 4.1.

## 4. Results and Discussion

### 4.1. ANOVA and regression equation of Ra

ANOVA technique helps in identifying the most influencing factor affecting the output parameter(Ra).The technique uses sum of squares and variance during analysis. Least squares technique is used in this approach. Table 4 shows the input factor levels and input values

Table 4 shows the variance of analysis for Ra.

Table 4.: Variace analysis for Ra

Source	DF	Adj SS	Adj MS	F-Value	P-Val
Model	9	6.63904	0.73767	10.59	0
Linear	3	4.75123	1.58374	22.73	0
Ton	1	0.04176	0.04176	0.6	0.449
Toff	1	0.43556	0.43556	6.25	0.023
Ip	1	4.27391	4.27391	61.34	0
Square	3	1.21507	0.40502	5.81	0.006
Ton*Ton	1	0.89218	0.89218	12.8	0.002
Toff*Toff	1	0.01357	0.01357	0.19	0.665
Ip*Ip	1	0.30933	0.30933	4.44	0.05
2-Way	3	0.67274	0.22425	3.22	0.049
Ton*Toff	1	0.67071	0.67071	9.63	0.006
Ton*Ip	1	0.00066	0.00066	0.01	0.924
Toff*Ip	1	0.00137	0.00137	0.02	0.89
Error	17	1.18447	0.06967		
Total	26	7.82351			

The surface parameters ( $R_a$ ) is predicted using input values of  $Ton$ ,  $Toff$ ,  $Ip$

$$\begin{aligned}
 R_a = & 3.27 + 0.744 \cdot Ton - 0.302 \cdot Toff - 0.0418 \cdot Ip \\
 & - 0.0964 \cdot Ton^2 + 0.0119 \cdot Toff^2 + 0.00227 \cdot Ip^2 \\
 & + 0.0591 \cdot Ton \cdot Toff + 0.00037 \cdot Ton \cdot Ip - 0.00053 \cdot Toff \cdot Ip
 \end{aligned} \tag{10}$$

#### 4.2. RSM surface plots

Figure 9 shows that as value of  $Ton$  increases  $R_a$  is increased but the increase is not significant, whereas it is significant when value of  $Toff$  is increased

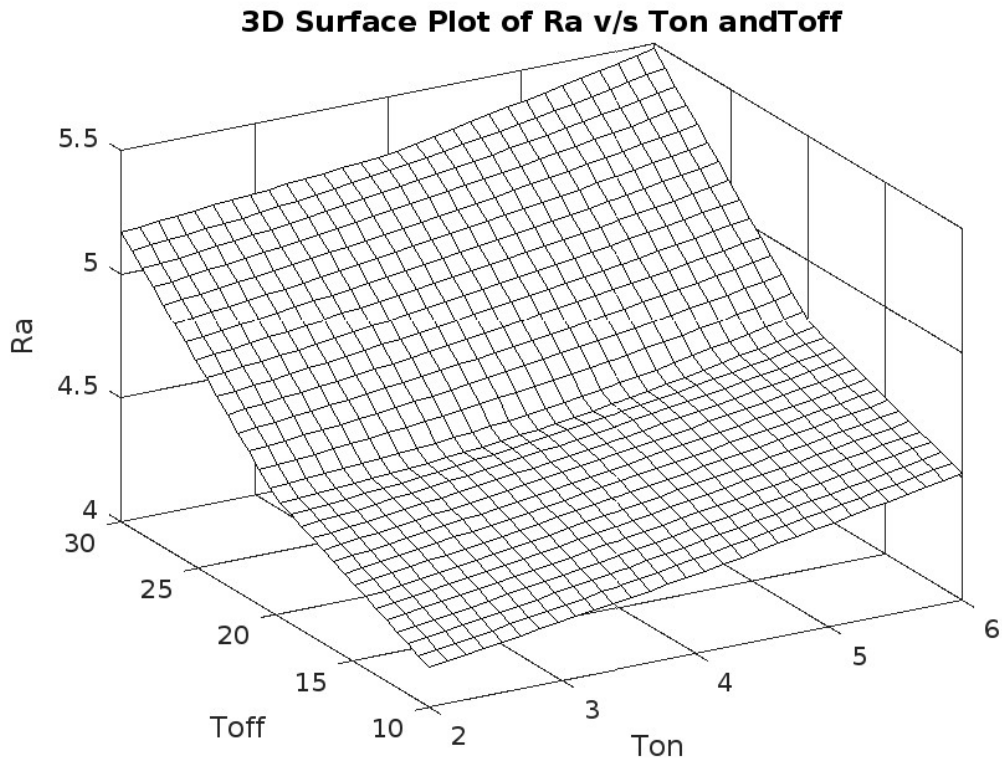


Figure 9.: 3D Plot Ra v/s Toff,Ton

Figure 10 shows that as value of  $Ton$  increases  $R_a$  is increased but the increase is not significant, whereas it is significant when value of  $Ip$  is increased

Figure 4.2 shows that as value of  $Toff$  increases  $R_a$  is not increasing significantly. When value of  $Ip$  is increasing  $R_a$  is also increasing fast. It indicates that value of peak current affects surface roughness  $R_a$  significantly.

**3D Surface Plot of Ra v/s Ton and Ip**

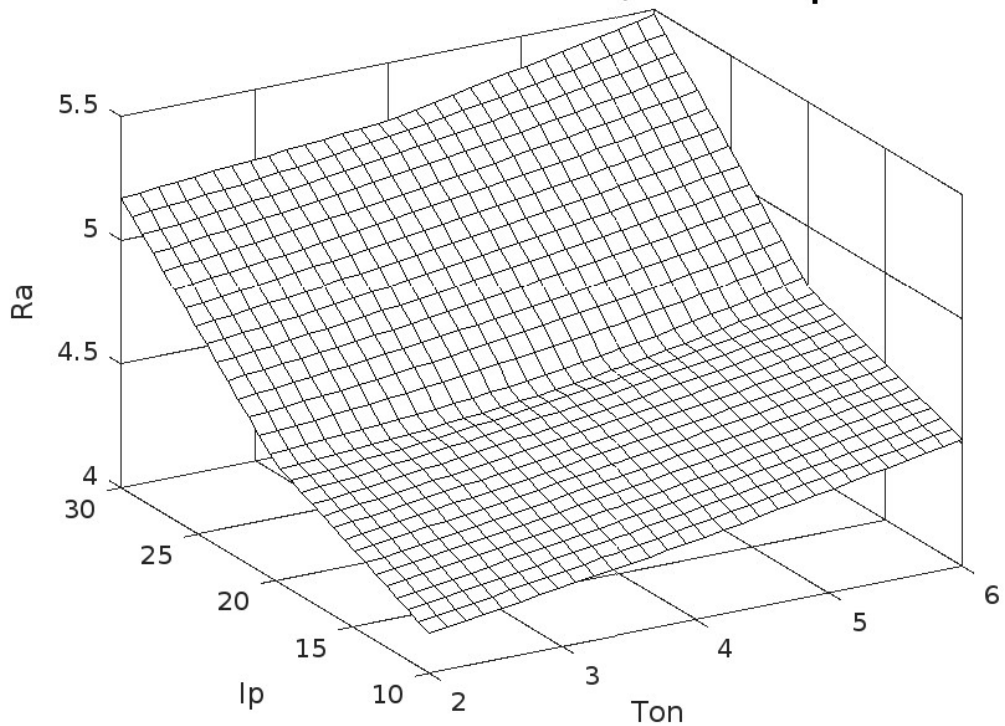


Figure 10.: 3D Plot of Ra v/s Ton, Ip

**3D Surface Plot of Ra v/s Toff and Ip**

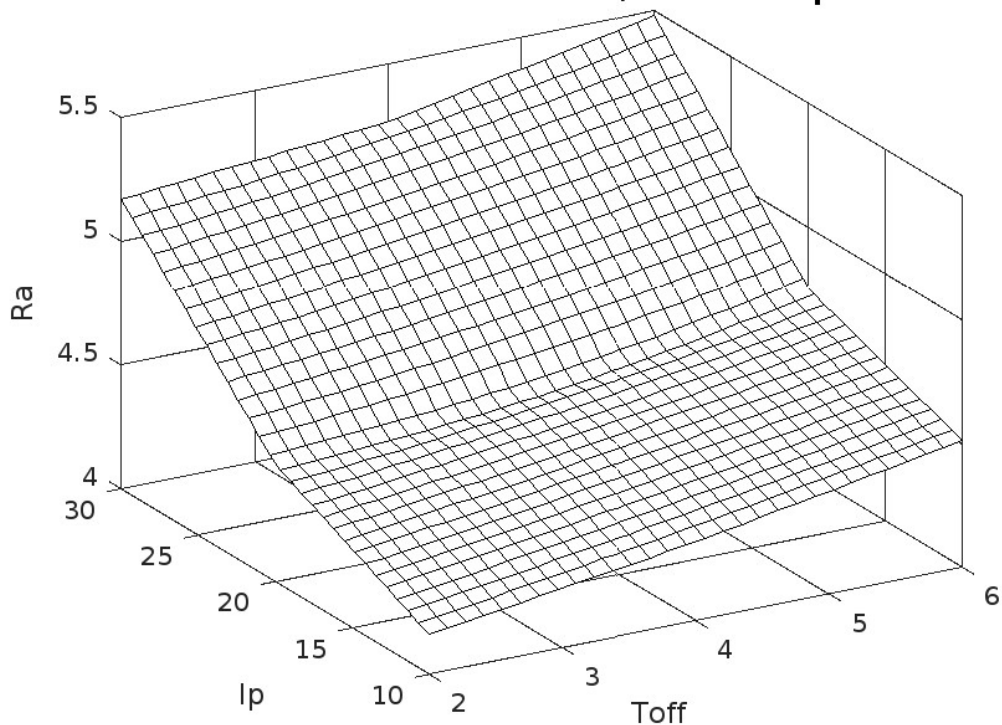


Figure 11.: 3D Plot of Ra v/s Toff, Ip

Figure 12 is bar chart of comparison of actual Ra-values and predicted Ra values. both the values are in proximity, showing strength of RSM model.

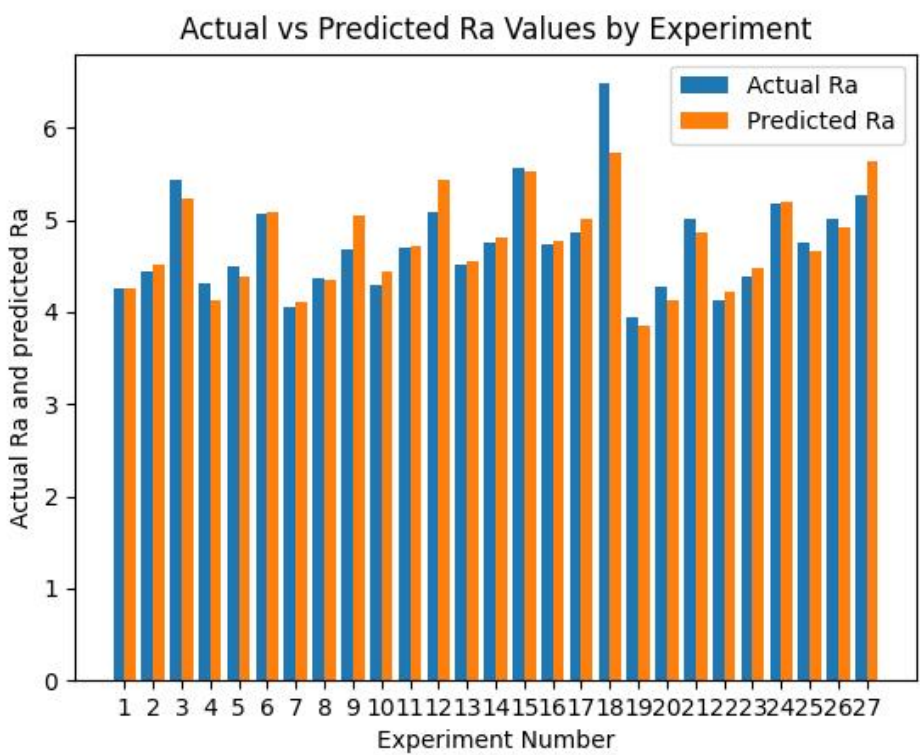


Figure 12.: Comparative graph of RSM for actual and predicted values of surface roughness

#### 4.3. Response surface method (RSM) results

Table 5.: RSM Retrue

Exp	Input factors			Experiment Output variables					Predicted output variables				
No	Ton	Toff	Ip	Ra	Rq	Rz	Rp	Rv	pRa	pRq	pRz	pRp	pRv
1	3	2	10	4.252	5.585	28.935	12.071	16.865	4.247	5.527	27.770	11.700	16.042
2	3	2	20	4.442	5.664	26.886	10.423	16.462	4.511	5.834	27.860	12.020	15.693
3	3	2	30	5.428	6.928	29.213	14.856	14.356	5.228	6.636	29.200	13.300	15.857
4	3	4	10	4.317	5.309	24.604	10.612	13.992	4.130	5.117	24.420	9.640	14.627
5	3	4	20	4.489	5.518	25.570	10.429	14.141	4.382	5.472	25.110	10.400	14.448
6	3	4	30	5.061	6.529	29.292	13.338	15.954	5.089	6.323	27.060	12.130	14.783
7	3	6	10	4.047	5.047	23.099	9.117	13.982	4.107	5.023	22.920	9.740	13.138
8	3	6	20	4.372	5.399	23.959	12.019	11.940	4.349	5.427	24.220	10.950	13.129
9	3	6	30	4.681	5.705	23.789	10.131	13.658	5.045	6.325	26.780	13.110	13.633
10	5	2	10	4.296	5.735	27.909	14.507	13.402	4.437	5.863	28.190	13.100	15.170
11	5	2	20	4.706	6.136	27.858	11.558	16.300	4.708	6.137	28.390	13.120	15.233
12	5	2	30	5.077	6.450	29.005	12.618	16.388	5.433	6.905	29.850	14.110	15.810
13	5	4	10	4.506	5.695	25.707	9.887	15.820	4.556	5.761	26.430	11.290	15.107
14	5	4	20	4.761	5.803	25.066	10.824	14.242	4.816	6.083	27.240	11.750	15.340
15	5	4	30	5.561	6.807	28.956	13.056	15.900	5.530	6.900	29.310	13.180	16.087
16	5	6	10	4.742	5.915	26.665	12.601	14.064	4.770	5.976	26.530	11.640	14.969
17	5	6	20	4.864	6.344	27.857	11.205	16.651	5.019	6.346	27.950	12.540	15.372
18	5	6	30	6.480	8.296	35.502	18.892	16.610	5.723	7.210	30.630	14.410	16.289
19	7	2	10	3.936	4.971	22.736	9.606	13.130	3.856	4.992	23.990	11.820	12.248
20	7	2	20	4.278	5.611	27.583	15.535	12.048	4.134	5.232	24.310	11.550	12.723
21	7	2	30	5.007	6.013	25.309	11.770	13.539	4.867	5.966	25.880	12.240	13.712
22	7	4	10	4.133	5.202	24.117	11.084	13.033	4.211	5.198	23.840	10.260	13.536
23	7	4	20	4.389	5.409	24.965	10.593	14.372	4.479	5.486	24.760	10.430	14.182
24	7	4	30	5.177	6.337	26.830	10.833	15.997	5.200	6.269	26.940	11.560	15.341
25	7	6	10	4.746	5.719	25.865	10.565	15.300	4.661	5.721	25.540	10.860	14.750
26	7	6	20	5.016	6.190	27.160	11.631	15.530	4.918	6.057	27.070	11.470	15.566
27	7	6	30	5.274	6.357	27.608	11.603	16.004	5.629	6.888	29.860	13.040	16.895

- The two-stage effort of obtaining a Surface Roughness (SR) model by RSM and optimization of this model, have resulted in a fairly useful method of obtaining process parameters in order to attain the improved surface quality.
- The investigation indicates that the discharge current, pulse-on time and pulse-off time are the primary factors influencing the SR of EDM8 material during EDM machining.
- Pulse-on time is found to be the dominant parameter influencing surface roughness.
- An increase in discharge current(Ip) was also observed to increase the roughness of the surface. The confirmation test showed that developed models can predict the SR accurately within 95% confidence interval.
- The methodology adopted establishes the optimization and hence facilitates the effective use of EDM machinable EN8 in industrial applications.

Results of RSM method are summarised in Table 39 for  $R^2$  and Table 38 100-MAPE. It is observed that values are comparatively lower than that in Table 37

#### 4.4. Artificial Neural Network results :

ANN model utilized Levenberg Marquadt (LM) optimizer, while predicting the surface roughness parameters. MSE, 100-MAPE, R<sup>2</sup>, were determined to assess the performance of the model while computing Ra,Rq,Rz,Rp,Rv roughness parameters.

##### 4.4.1. Levenberg Marquadt (LM)

Different ANN architectures (3,3,5) to (3,10,5) were assessed during the research. Here, (3,3,5) architecture means an ANN with 3 Input layers, 3 Hidden layers and 5 output layers. Table 9, 11 and 13 show the results obtained through ANN model for training. Table 9 gives the MSE values in predicting surface roughness . Similarly table 11 and table 13 show the 100-MAPE and R<sup>2</sup> respectively. Table 10, 12 and 14 show MSE, 100-MAPE ans R<sup>2</sup> respectively during testing.

Table 6.: MSE - Training

Model	Ra	Rq	Rz	Rp	Rv	Model	Ra	Rq	Rz	Rp	Rv
3,3,5	0.6145	0.5268	12.7484	5.7805	1.9906	0.8816	0.6776	13.3610	10.9872	1.7374	
3,4,5	0.2320	0.3116	5.7632	3.3648	1.5589	0.2875	0.5838	11.6035	7.7585	2.7788	
3,5,5	0.2577	0.3769	5.6313	4.1938	1.6742	0.2320	0.4469	15.8244	7.5464	2.8476	
3,6,5	0.2611	0.3980	5.8941	4.3860	1.7359	0.3246	0.5137	7.2145	4.4629	2.7386	
3,7,5	0.3598	0.3524	5.1894	3.7249	1.7618	0.3732	0.4807	9.1344	5.6403	1.9395	
3,8,5	0.4466	0.5745	9.0193	5.1845	2.2094	0.4320	0.6740	10.2400	7.4878	2.7025	
3,9,5	0.2267	0.4160	4.8924	3.4021	1.7225	0.3072	0.4975	9.3864	5.9403	2.4214	
3,10,5	0.5112	0.5755	6.4854	5.1552	2.1182	0.3583	0.5034	8.1824	5.4917	2.6757	

Table 8.: 100-MAPE - Training

Table 7.: MSE - Testing

Table 9.: 100-MAPE-Testing

Model	Ra	Rq	Rz	Rp	Rv	Model	Ra	Rq	Rz	Rp	Rv
3,3,5	89.4593	91.3179	91.4111	86.4767	92.1775	86.7293	89.5728	90.0064	79.0522	92.7297	
3,4,5	92.3164	93.3200	93.5700	88.9384	93.3983	91.4049	90.9243	90.6595	83.7028	90.0244	
3,5,5	91.9950	92.3777	94.0158	88.5328	93.2417	92.2612	91.4242	89.8107	84.6160	90.1505	
3,6,5	91.7527	92.0989	93.2501	88.1002	92.2379	90.8824	91.6115	92.6710	87.6929	90.5660	
3,7,5	90.5230	93.0120	94.3972	89.7952	92.1567	89.8605	91.7290	91.8469	86.2687	91.4846	
3,8,5	88.6511	90.5537	91.5667	86.1443	92.1446	88.2478	88.5413	89.9262	80.5972	90.4051	
3,9,5	92.6582	91.9939	94.3163	89.5222	92.6677	91.4528	90.9285	91.0559	85.6070	90.6770	
3,10,5	90.0553	90.5693	92.9260	87.0656	91.6169	90.7455	92.0504	91.6534	87.3093	90.2720	

Table 10.: R<sup>2</sup> - Training

Table 11.: R<sup>2</sup> - Testing

model	Ra	Rq	Rz	Rp	Rv	model	Ra	Rq	Rz	Rp	Rv
3,3,5	97.3125	98.5430	98.2424	96.0009	99.1047	96.1432	98.1774	98.1592	92.4814	99.2417	
3,4,5	98.9802	99.1304	99.2027	97.7187	99.2958	98.7373	98.3834	98.4129	94.8385	98.7364	
3,5,5	98.8711	98.9524	99.2246	97.1506	99.2439	99.0192	98.7908	97.8311	95.0236	98.7175	
3,6,5	98.8594	98.8940	99.1891	97.0186	99.2130	98.6094	98.6718	99.0452	97.1497	98.7152	
3,7,5	98.4280	99.0220	99.2810	97.4483	99.2045	98.4467	98.7549	98.7688	96.4110	99.1228	
3,8,5	98.0326	98.3923	98.7486	96.4500	98.9990	98.1316	98.1550	98.5770	94.9701	98.7780	
3,9,5	99.0059	98.8388	99.3193	97.6813	99.2155	98.7123	98.6582	98.7163	96.1578	98.8921	
3,10,5	97.7623	98.4061	99.1010	96.4899	99.0421	98.4620	98.6382	98.8616	96.5370	98.7453	

Perfomance of different networks trained and tested with GD, GDA,LN and RProp algorithm are presented in table 37. Considering results of comparison metric 100-MAPE, accuracy of CNN trained model from the table, it is seen that prediction of different types of surface roughness of EDM component of EN8 are affected with different architecture of optimisers which summerised below.

- Average roughness (Ra) is

Table 12.: Result of 100-MAPE and R-squared for ANOVA

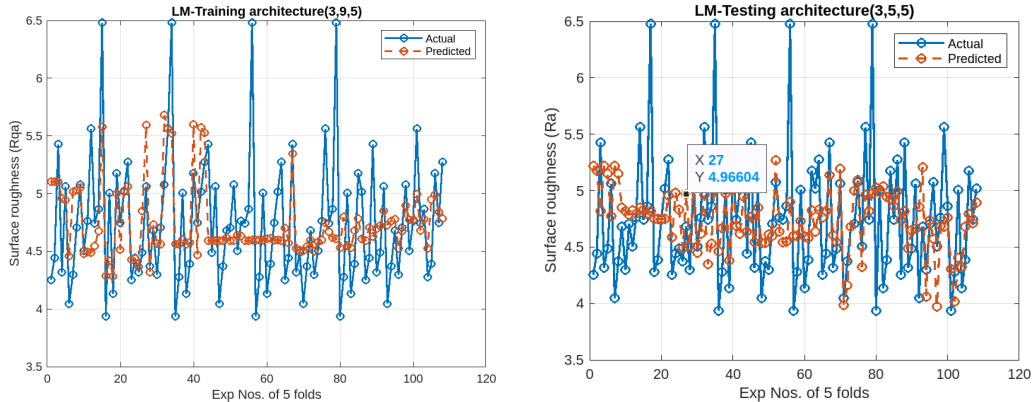
100-MAPE					R-Squared				
Ra	Rq	Rz	Rp	Rv	Ra	Rq	Rz	Rp	Rv
97.2563	97.0520	96.4014	89.6507	94.9921	99.8075	99.7379	99.6679	98.1065	99.6734

Table 13.: ANN result of  $R^2$  with optimizers

Ra		Rq		Rz		Rp		Rv	
Train	Test								
99.0059	99.0192	98.8806	99.1304	99.4371	99.3314	97.8093	97.2680	99.2958	99.2417
LM	LM	LM	GDA	GD	GD	GD	RProp	LM	LM

Table 14.: ANN result of 100-MAPE with optimizers

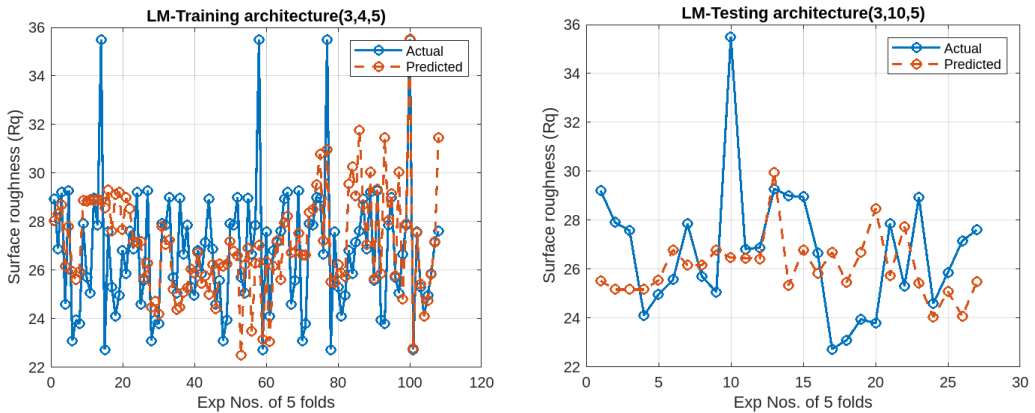
	Ra		Rq		Rz		Rp		Rv	
	Train	Test								
	92.6582	92.2612	93.3200	92.2612	95.1854	93.5771	90.1051	89.4264	93.3983	92.7297
Optimizer	LM	LM	LM	LM	GD	GD	GD	GDA	LM	LM



(a) LM optimiser with architecture (3,9,5) of Training

(b) LM optimiser with architecture (3,5,5) of testing

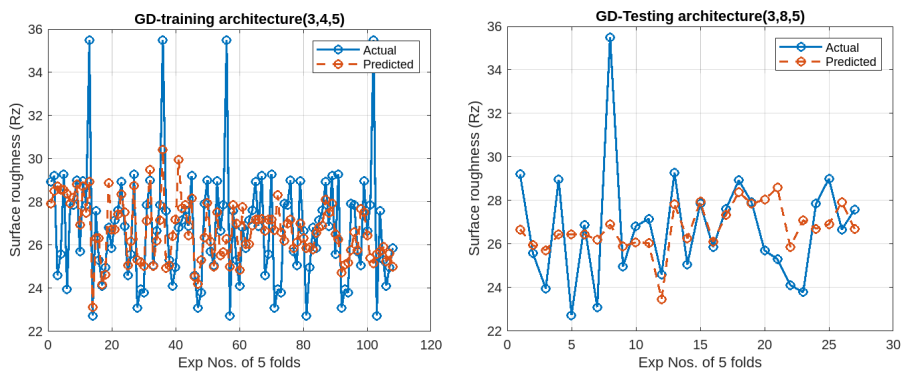
Figure 13.: Chart of highest value of 100-MAPE for Ra



(a) LM optimiser with architecture (3,4,5) of Training

(b) LM optimiser with architecture (3,10,5) of testing

Figure 14.: Chart of highest value of 100-MAPE for Rq



(a) GD optimiser with architecture (3,4,5) of Training

(b) GD optimiser with architecture (3,8,5) of testing

Figure 15.: Chart of highest value of 100-MAPE for Rz

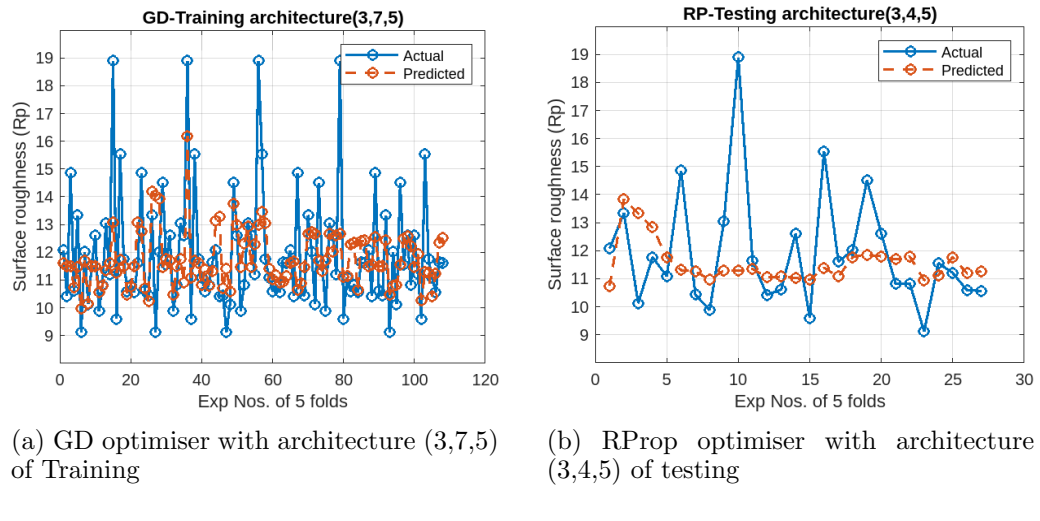


Figure 16.: Chart of highest value of 100-MAPE for Rp

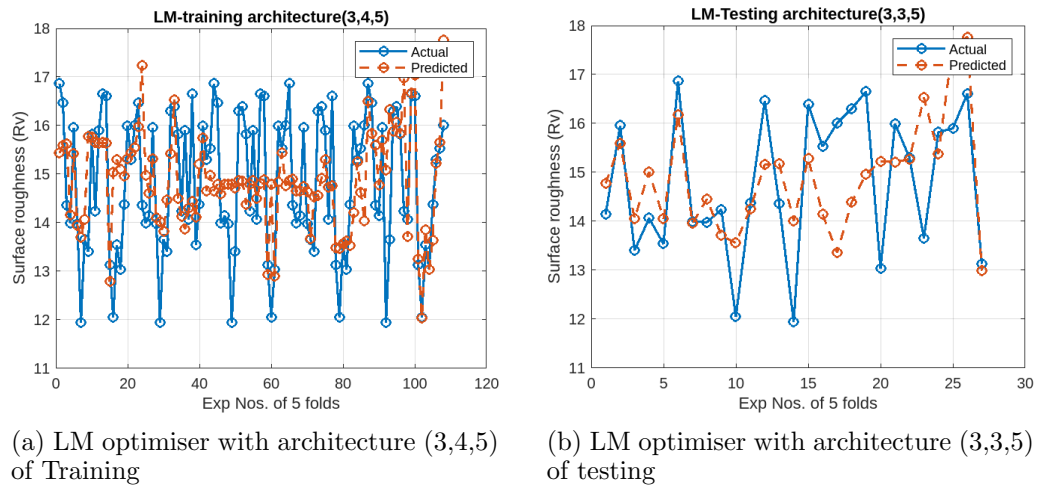


Figure 17.: Chart of highest value of 100-MAPE for Rv

## 5. Conclusion

It is concluded from the results that the Levenberg-Marquardt (LM) algorithm has an accuracy using Training and testing results of MAPE and R<sub>2</sub> is around 92% and 97% respectively for surface roughness Ra, Rq and R<sub>v</sub> while R<sub>z</sub> follows Gradient Descent (GD) and Root mean squared Prop (RProp) follows partially GD and RProp algorithms. The study proposes a deep learning-based method employing images of die-sinking EDM-machined work piece surfaces. Looking at these pictures captured by a CCD camera, the recommended method may accurately predict surface roughness values comparable to those acquired by a profilometer. With the help of this integrated technique, operators can measure roughness values that correspond to goal specifications on designs. Additionally, the learning-based technique shows promise for characterizing surface morphology and enabling automatic in-situ quality control in intelligent manufacturing cells, applicable to both EDM machining and other machining processes.

## References

- [1] Anurag Joshi, Amit Kumar Saraf, and Ravi Kumar Goyal. Edm machining of die steel en8 and testing of surface roughness with varying parameters. *Materials Today: Proceedings*, 28:2557–2560, 2020.
- [2] Madhumitha Ravichandran, Guanyu Su, Chi Wang, Jee Hyun Seong, Artyom Kossolapov, Bren Phillips, Md Mahamudur Rahman, and Matteo Bucci. Decrypting the boiling crisis through data-driven exploration of high-resolution infrared thermometry measurements. *Applied Physics Letters*, 118(25), 2021.
- [3] M Mustafaiz Ahmad, R Davis, N Maurya, P Singh, and S Gupta. Optimization of process parameters in electric discharge machining process. *International Journal of Mechanical Engineering (IJME)*, 5(4):45–52, 2016.
- [4] Ushasta Aich and Simul Banerjee. Modeling of edm responses by support vector machine regression with parameters selected by particle swarm optimization. *Applied Mathematical Modelling*, 38(11-12):2800–2818, 2014.
- [5] C Balasubramaniyan, K Rajkumar, and S Santosh. Wire-edm machinability investigation on quaternary ni44ti50cu4zr2 shape memory alloy. *Materials and Manufacturing Processes*, 36(10):1161–1170, 2021.
- [6] Milan Kumar Das, Kaushik Kumar, Tapan Kumar Barman, and Prasanta Sahoo. Prediction of surface roughness in edm using response surface methodology and artificial neural network. *Journal of Manufacturing Technology Research*, 6(3/4):93, 2014.
- [7] Alessandro Giusti, Matteo Dotta, Umang Maradia, Marco Boccadoro, Luca M Gambardella, and Adriano Nasciuti. Image-based measurement of material roughness using machine learning techniques. *Procedia CIRP*, 95:377–382, 2020.
- [8] Ashish Goyal, Adithya Garimella, and Priyanka Saini. Optimization of surface roughness by design of experiment techniques during wire edm machining. *Materials Today: Proceedings*, 47:3195–3197, 2021.
- [9] C Naresh, PSC Bose, and CSP Rao. Artificial neural networks and adaptive neuro-fuzzy models for predicting wedm machining responses of nitinol alloy: Comparative study. *SN Applied Sciences*, 2:1–23, 2020.
- [10] Je-Kang Park, Bae-Keun Kwon, Jun-Hyub Park, and Dong-Joong Kang. Machine learning-based imaging system for surface defect inspection. *International Journal*

*of Precision Engineering and Manufacturing-Green Technology*, 3:303–310, 2016.

- [11] KM Patel\*, Pulak M Pandey, and P Venkateswara Rao. Determination of an optimum parametric combination using a surface roughness prediction model for edm of al2o3/sicw/tic ceramic composite. *Materials and Manufacturing Processes*, 24(6):675–682, 2009.
- [12] Dhiren R Patel, Vinay Vakharia, and Mysore B Kiran. Texture classification of machined surfaces using image processing and machine learning techniques. *FME Transactions*, 47(4):865–872, 2019.
- [13] Uma Maheshwera Reddy Paturi, Suryapavan Cheruku, Venkat Phani Kumar Pasunuri, Sriteja Salike, NS Reddy, and Srija Cheruku. Machine learning and statistical approach in modeling and optimization of surface roughness in wire electrical discharge machining. *Machine Learning with Applications*, 6:100099, 2021.
- [14] TR Paul, A Saha, H Majumder, V Dey, and P Dutta. Multi-objective optimization of some correlated process parameters in edm of inconel 800 using a hybrid approach. *Journal of the Brazilian Society of Mechanical Sciences and Engineering*, 41:1–11, 2019.
- [15] BC Routara, Diptikanta Das, MP Satpathy, BK Nanda, AK Sahoo, and Shubham S Singh. Investigation on machining characteristics of t6-al7075 during edm with cu tool in steady and rotary mode. *Materials Today: Proceedings*, 26:2143–2150, 2020.
- [16] Jamal Saeedi, Matteo Dotta, Andrea Galli, Adriano Nasciuti, Umang Maradia, Marco Boccadoro, Luca Maria Gambardella, and Alessandro Giusti. Measurement and inspection of electrical discharge machined steel surfaces using deep neural networks. *Machine Vision and Applications*, 32:1–15, 2021.
- [17] DM Shivanna, MB Kiran, and SD Kavitha. Evaluation of 3d surface roughness parameters of edm components using vision system. *Procedia Materials Science*, 5:2132–2141, 2014.
- [18] Ranjit Singh, Ravi Pratap Singh, and Rajeev Trehan. Machine learning algorithms based advanced optimization of edm parameters: An experimental investigation into shape memory alloys. *Sensors International*, 3:100179, 2022.
- [19] Mustafa Ulas, Osman Aydur, Turan Gurgenc, and Cihan Ozel. Surface roughness prediction of machined aluminum alloy with wire electrical discharge machining by different machine learning algorithms. *Journal of Materials Research and Technology*, 9(6):12512–12524, 2020.
- [20] Vinay Vakharia, Jay Vora, Sakshum Khanna, Rakesh Chaudhari, Milind Shah, Danil Yu Pimenov, Khaled Giasin, Parth Prajapati, and Szymon Wojciechowski. Experimental investigations and prediction of wedmed surface of nitinol sma using singan and densenet deep learning model. *journal of materials research and technology*, 18:325–337, 2022.
- [21] H Varol Ozkavak, MM Sofu, B Duman, and S Bacak. Estimating surface roughness for different edm processing parameters on inconel 718 using gep and ann. *cirp j manuf sci technol* 33: 306–314, 2021.
- [22] L Yogesh, M Arunadevi, and CPS Prakash. Predicton of mrr & surface roughness in wire edm machining using decision tree and naive bayes algorithm. In *2021 International Conference on Emerging Smart Computing and Informatics (ESCI)*, pages 527–532. IEEE, 2021.
- [23] Wang Zhang, Chunwang Luo, Qingyuan Ma, Zhenqiang Lin, Lan Yang, Jun Zheng, Xiaohong Ge, Wei Zhang, Yuangang Liu, and Jumei Tian. Prediction model of surface roughness of selective laser melting formed parts based on back propagation neural network. *Engineering Reports*, 5(12):e12570, 2023.

- [24] J Kundrák, I Sztankovics, and V Molnár. Accuracy and topography analysis of hard machined surfaces. *Manufacturing Technology*, 21(4):512–519, 2021.
- [25] İlhan Asiltürk and Mehmet Çunkaş. Modeling and prediction of surface roughness in turning operations using artificial neural network and multiple regression method. *Expert systems with applications*, 38(5):5826–5832, 2011.

## 6. Supplementary information

### 6.1. Declaration

- The authors have no relevant financial or non-financial interests to disclose.
- The authors have no conflicts of interest to declare that are relevant to the content of this article.
- All authors certify that they have no affiliations with or involvement in any organization or entity with any financial interest or non-financial interest in the subject matter or materials discussed in this manuscript.
- The authors have no financial or proprietary interest in the material discussed in this article.

#### 6.1.1. Funding

The authors did not receive funding from any organization for the submitted work. Also, the authors declare they have no financial interests. Therefore, the authors have no relevant financial or non-financial interests to disclose.

#### 6.1.2. Conflicts of interest/Competing interests

There are not any Conflicts of interest and Competing interests about the presented results in this paper. All results are based on laboratory data and based on common statistical criteria in the scientific articles.

### 6.2. Availability of data and material

All of data and material are presented in Figures

#### 6.2.1. Code availability

[Visit Github](#)

## 7. Annexure : I

Table 15.: ANOVA -  $R_v$

Source	DF	Adj SS	Adj MS	F-Value	P-Value
Model	9	38.4628	4.2736	4.64	0.004
Linear	3	2.4327	0.8109	0.88	0.472
Ton	1	0.3192	0.3192	0.35	0.564
Toff	1	0.1063	0.1063	0.12	0.739
Ip	1	1.9239	1.9239	2.09	0.168
Square	3	10.1324	3.3775	3.66	0.035
Ton*Ton	1	9.4514	9.4514	10.25	0.006
Toff*Toff	1	0.0732	0.0732	0.08	0.782
Ip*Ip	1	0.9629	0.9629	1.04	0.322
2-Way Interaction	3	25.6187	8.5396	9.26	0.001
Ton*Toff	1	21.924	21.924	23.78	0
Ton*Ip	1	2.0402	2.0402	2.21	0.156
Toff*Ip	1	1.6544	1.6544	1.79	0.199
Error	16	14.7494	0.9218		
Total	25	53.2122			

Table 16.: ANOVA -  $R_q$

Model	9	9.9123	1.10136	7.37	0
Linear	3	6.027	2.009	13.45	0
Ton	1	0.0009	0.00087	0.01	0.94
Toff	1	0.1961	0.19615	1.31	0.268
Ip	1	5.83	5.82997	39.04	0
Square	3	2.7048	0.90161	6.04	0.005
Ton*Ton	1	2.1877	2.18769	14.65	0.001
Toff*Toff	1	0.1501	0.1501	1.01	0.33
Ip*Ip	1	0.367	0.36704	2.46	0.135
2-Way Interaction	3	1.1805	0.39349	2.63	0.083
Ton*Toff	1	1.139	1.13898	7.63	0.013
Ton*Ip	1	0.0137	0.01374	0.09	0.765
Toff*Ip	1	0.0277	0.02774	0.19	0.672
Error	17	2.539	0.14935		
Total	26	12.4512			

$$\begin{aligned}
 R_v = & 19.45 + 1.48 \cdot \text{Ton} - 2.348 \cdot \text{Toff} - 0.310 \cdot \text{Ip} \\
 & - 0.331 \cdot \text{Ton}^2 + 0.0280 \cdot \text{Toff}^2 + 0.00406 \cdot \text{Ip}^2 \\
 & + 0.3379 \cdot \text{Ton} \cdot \text{Toff} + 0.0206 \cdot \text{Ton} \cdot \text{Ip} + 0.0197 \cdot \text{Toff} \cdot \text{Ip} \\
 & \quad (11a) \\
 R_q = & 4.13 + 1.239 \cdot \text{Ton} - 0.697 \cdot \text{Toff} - 0.0432 \cdot \text{Ip} \\
 & - 0.1510 \cdot \text{Ton}^2 + 0.0395 \cdot \text{Toff}^2 + 0.00247 \cdot \text{Ip}^2 \\
 & + 0.0770 \cdot \text{Ton} \cdot \text{Toff} - 0.00169 \cdot \text{Ton} \cdot \text{Ip} + 0.00240 \cdot \text{Toff} \cdot \text{Ip} \\
 & \quad (11b)
 \end{aligned}$$

Table 17.: ANOVA - Rz

Source	DF	Adj SS	Adj MS	F-Value	P-Value
Model	9	113.408	12.6009	3.31	0.016
Linear	3	38.59	12.8633	3.38	0.043
Ton	1	0.56	0.5597	0.15	0.706
Toff	1	0.858	0.8581	0.23	0.641
Ip	1	37.172	37.1723	9.76	0.006
Square	3	39.498	13.1659	3.46	0.04
Ton*Ton	1	31.94	31.9396	8.38	0.01
Toff*Toff	1	5.179	5.1795	1.36	0.26
Ip*Ip	1	2.378	2.3785	0.62	0.44
2-Way Interaction	3	35.32	11.7735	3.09	0.055
Ton*Toff	1	30.694	30.6944	8.06	0.011
Ton*Ip	1	0.157	0.1571	0.04	0.841
Toff*Ip	1	4.469	4.4689	1.17	0.294
Error	17	64.768	3.8099		
Total	26	178.176			

$$\begin{aligned}
 R_z = & 28.07 + 3.97 \cdot \text{Ton} - 4.58 \cdot \text{Toff} - 0.259 \cdot \text{Ip} \\
 & - 0.577 \cdot \text{Ton}^2 + 0.232 \cdot \text{Toff}^2 + 0.00630 \cdot \text{Ip}^2 \\
 & + 0.400 \cdot \text{Ton} \cdot \text{Toff} + 0.0057 \cdot \text{Ton} \cdot \text{Ip} + 0.0305 \cdot \text{Toff} \cdot \text{Ip} \\
 & \quad (12\text{a})
 \end{aligned}$$

$$\begin{aligned}
 R_p = & 9.80 + 3.40 \cdot \text{Ton} - 3.05 \cdot \text{Toff} - 0.113 \cdot \text{Ip} \\
 & - 0.334 \cdot \text{Ton}^2 + 0.269 \cdot \text{Toff}^2 + 0.00484 \cdot \text{Ip}^2 \\
 & \quad (12\text{b})
 \end{aligned}$$

### 7.1. Gradient Descent (GD)- Training

675768978

Table 19.: MSE

Model	R <sub>a</sub>	R <sub>q</sub>	R <sub>z</sub>	R <sub>p</sub>	R <sub>v</sub>
3,3,5	0.7779	0.6526	8.9445	5.0344	2.6556
3,4,5	0.4567	0.5673	4.1124	4.0411	1.7583
3,5,5	1.1804	1.5216	8.1971	4.3706	2.7105
3,6,5	0.6347	0.5138	5.5654	3.5982	1.8931
3,7,5	0.5741	0.7259	4.0850	3.2085	1.8164
3,8,5	0.5001	0.6199	5.4799	4.1741	1.5646
3,9,5	0.3782	0.6075	5.8608	4.9034	2.2457
3,10,5	0.6918	1.4944	10.5247	3.9914	3.1305
	85.7883	90.1561	92.2319	86.7311	90.8281
	88.4859	90.1404	95.1854	88.8411	92.8531
	79.8802	83.1496	91.9165	87.6554	90.5394
	87.3674	90.9756	93.7972	88.8870	91.6324
	87.7135	89.5326	94.8920	90.1051	92.2929
	88.2882	89.8521	93.5099	88.2318	92.8523
	89.6233	90.6317	93.5365	88.3377	91.8186
	86.0773	82.1994	91.1631	88.4650	89.8138
	96.5865	98.1760	98.7620	96.5599	98.7995
	97.9862	98.4038	99.4296	97.2432	99.2045
	94.8035	95.7435	98.8650	97.0206	98.7761
	97.2252	98.5673	99.2338	97.5618	99.1450
	97.5024	98.0022	99.4371	97.8093	99.1789
	97.8201	98.2755	99.2423	97.1409	99.2963
	98.3460	98.3005	99.1898	96.6527	98.9837
	96.9812	95.8205	98.5489	97.2733	98.5797

Table 20.: 100-MAPE

Table 21.: R2

#### 7.1.1. Gradient Descent (GD) - Testing

Table 22.: MSE

Model	R <sub>a</sub>	R <sub>q</sub>	R <sub>z</sub>	R <sub>p</sub>	R <sub>v</sub>
3,3,5	0.6399	0.5559	6.8759	5.0609	3.1432
3,4,5	0.4825	0.9724	10.4342	5.9997	3.0682
3,5,5	1.3236	1.8588	10.7660	5.7609	4.0829
3,6,5	0.6048	0.7407	6.2316	5.0843	1.8011
3,7,5	0.5005	0.5593	4.9362	4.5105	2.2328
3,8,5	0.4051	0.7107	5.2199	4.6831	3.8228
3,9,5	0.5983	0.9236	10.9822	6.8305	3.1814
3,10,5	0.6354	1.2557	10.8485	4.3429	4.1827
	87.2777	90.7939	92.5721	86.8403	89.6754
	89.0851	86.3763	90.2636	85.4969	90.2163
	77.5439	81.2870	90.5205	85.5367	88.7338
	86.0146	89.1525	93.2920	86.7215	92.4535
	88.3628	90.2443	93.5032	87.7668	91.2777
	89.1217	89.0986	93.5771	86.8903	88.7149
	87.8631	88.3081	90.4847	85.2551	89.2708
	85.2942	83.2422	90.9524	88.2682	88.6183
	97.1133	98.4715	99.0805	96.7969	98.5642
	97.9642	97.3715	98.5414	96.2305	98.6193
	94.2286	94.9256	98.5454	96.3924	98.0809
	97.3555	98.0643	99.1841	96.8731	99.1821
	97.7797	98.4475	99.3314	96.9629	98.9535
	98.2255	98.1102	99.2850	96.8717	98.2787
	97.4526	97.6421	98.5146	96.0925	98.5248
	97.1626	96.4773	98.5020	97.1350	98.1202

Table 21.: R2

Table 23.: 100-MAPE

Table 24.: R<sup>2</sup>

### 7.1.2. Gradient Descent Adaptive (GDA)- Training

Table 25.: MSE

Model	Ra	Rq	Rz	Rp	Rv
3,3,5	0.5686	1.0356	5.4496	3.6828	2.9641
3,4,5	0.5300	0.6708	5.7447	4.0120	2.2133
3,5,5	0.4486	0.6838	5.2934	4.0257	2.1350
3,6,5	1.1633	1.3115	8.3433	4.7127	1.9791
3,7,5	0.3687	0.5137	5.6347	4.1389	2.4303
3,8,5	0.3335	0.4533	6.7832	3.9568	2.4064
3,9,5	1.0102	0.5114	5.6333	4.2942	2.1862
3,10,5	0.4894	0.4403	6.0374	3.9208	2.1189

Table 26.: 100-MAPE

Model	Ra	Rq	Rz	Rp	Rv
3,3,5	86.4528	86.3534	93.2940	87.6888	90.5958
3,4,5	88.4843	89.6484	93.7724	88.5469	91.3603
3,5,5	89.0898	89.2792	93.5208	88.4856	91.6212
3,6,5	82.7768	85.3713	92.2289	88.3244	91.5670
3,7,5	89.4719	90.5872	93.3861	88.5534	91.5162
3,8,5	90.1563	91.7614	93.1170	88.3436	90.9095
3,9,5	83.0843	90.3237	93.7372	87.1139	91.2153
3,10,5	88.2365	91.4493	93.1689	88.1133	91.1314

Table 27.: R<sup>2</sup>

Model	Ra	Rq	Rz	Rp	Rv
3,3,5	86.2255	81.3561	91.5968	83.2096	86.5399
3,4,5	89.8145	90.1799	92.7173	87.7070	90.4629
3,5,5	88.2345	89.9694	91.7693	84.2450	89.9527
3,6,5	80.6744	84.2998	88.5244	89.4264	90.6904
3,7,5	89.8009	89.8489	92.8793	88.5134	90.8829
3,8,5	90.3000	91.7128	92.6720	86.7530	89.8871
3,9,5	84.9822	92.0182	91.6488	86.1571	91.2591
3,10,5	90.8329	89.7613	91.4751	83.8114	90.9820

Table 28.: R<sup>2</sup>

Table 29.: 100-MAPE

Table 30.: MSE

#### 7.1.4. Resilient Backpropagation (*RProp*)- Training

Table 31.: MSE

Model	Ra	Rq	Rz	Rp	Rv
3,3,5	0.4054	0.4503	3.4458	2.4101	90.1411
3,4,5	0.2750	0.3780	5.1033	3.2810	2.0257
3,5,5	0.7747	0.5886	6.3194	5.7125	2.9942
3,6,5	0.4220	0.5742	6.0855	4.4157	2.7196
3,7,5	0.3055	0.5751	5.0551	4.1009	1.7572
3,8,5	0.3493	0.6995	5.9264	4.7299	2.1577
3,9,5	0.4623	0.5240	5.6926	4.4099	2.1416
3,10,5	0.3602	0.7306	6.6492	4.3102	2.2201

#### 7.1.5. Resilient Backpropagation (*RProp*) - Testing

Table 34.: MSE

Model	Ra	Rq	Rz	Rp	Rv
3,3,5	0.4737	0.5547	12.3075	11.5809	3.0096
3,4,5	0.3868	0.4548	7.2609	4.3790	2.6160
3,5,5	0.5372	0.5277	8.1677	5.5556	3.1009
3,6,5	0.4813	0.7669	9.5201	5.7815	2.9498
3,7,5	0.3966	0.6212	6.6503	4.4882	1.9346
3,8,5	0.4811	0.9717	8.2418	5.6460	2.1646
3,9,5	0.4332	0.4443	6.5408	5.8276	2.1740
3,10,5	0.3805	0.5641	7.6993	4.3662	2.1690

Table 32.: 100-MAPE

Model	Ra	Rq	Rz	Rp	Rv
3,3,5	0.4054	0.4503	3.48833	3.4458	2.4101
3,4,5	0.2750	0.3780	5.1033	3.2810	2.0257
3,5,5	0.7747	0.5886	6.3194	5.7125	2.9942
3,6,5	0.4220	0.5742	6.0855	4.4157	2.7196
3,7,5	0.3055	0.5751	5.0551	4.1009	1.7572
3,8,5	0.3493	0.6995	5.9264	4.7299	2.1577
3,9,5	0.4623	0.5240	5.6926	4.4099	2.1416
3,10,5	0.3602	0.7306	6.6492	4.3102	2.2201

Table 33.: R2

Model	Ra	Rq	Rz	Rp	Rv
3,3,5	0.4054	0.4503	3.48833	3.4458	2.4101
3,4,5	0.2750	0.3780	5.1033	3.2810	2.0257
3,5,5	0.7747	0.5886	6.3194	5.7125	2.9942
3,6,5	0.4220	0.5742	6.0855	4.4157	2.7196
3,7,5	0.3055	0.5751	5.0551	4.1009	1.7572
3,8,5	0.3493	0.6995	5.9264	4.7299	2.1577
3,9,5	0.4623	0.5240	5.6926	4.4099	2.1416
3,10,5	0.3602	0.7306	6.6492	4.3102	2.2201

Table 35.: 100-MAPE

Model	Ra	Rq	Rz	Rp	Rv
3,3,5	0.4054	0.4503	3.48833	3.4458	2.4101
3,4,5	0.2750	0.3780	5.1033	3.2810	2.0257
3,5,5	0.7747	0.5886	6.3194	5.7125	2.9942
3,6,5	0.4220	0.5742	6.0855	4.4157	2.7196
3,7,5	0.3055	0.5751	5.0551	4.1009	1.7572
3,8,5	0.3493	0.6995	5.9264	4.7299	2.1577
3,9,5	0.4623	0.5240	5.6926	4.4099	2.1416
3,10,5	0.3602	0.7306	6.6492	4.3102	2.2201

Table 36.: R<sup>2</sup>

Model	Ra	Rq	Rz	Rp	Rv
3,3,5	0.4054	0.4503	3.48833	3.4458	2.4101
3,4,5	0.2750	0.3780	5.1033	3.2810	2.0257
3,5,5	0.7747	0.5886	6.3194	5.7125	2.9942
3,6,5	0.4220	0.5742	6.0855	4.4157	2.7196
3,7,5	0.3055	0.5751	5.0551	4.1009	1.7572
3,8,5	0.3493	0.6995	5.9264	4.7299	2.1577
3,9,5	0.4623	0.5240	5.6926	4.4099	2.1416
3,10,5	0.3602	0.7306	6.6492	4.3102	2.2201

Table 37.: Comparison of results of optimizers

Optimizer	Maximum value of-(100-MAPE)					Maximum value of-R <sup>2</sup>				
	Ra	Rq	Rz	Rp	Rv	Ra	Rq	Rz	Rp	Rv
GD-Train Architecture	89.6233	90.9756	<b>95.1854</b> (3,4,5)	<b>90.1051</b> (3,7,5)	92.8531	98.3436	98.5673	<b>99.4371</b> (3,7,5)	<b>97.8093</b> (3,7,5)	99.2045
GD-Test Architecture	89.1217	90.7939	<b>93.5771</b> (3,8,5)	88.2682	92.4535	98.2255	98.4715	<b>99.3314</b> (3,7,5)	97.1350	99.1621
GDA-Train	90.1563	91.7614	93.7724	88.5534	91.6212	98.5452	98.7759	99.2662	97.4794	99.1045
GDA-Test Architecture	90.8329	92.0182	92.8793	<b>89.4264</b> (3,6,5)	91.2591	98.6352	<b>98.8806</b> (3,9,5)	99.1269	97.1419	98.9789
LM-Train Architecture	<b>92.6582</b> (3,9,5)	<b>93.3200</b> (3,4,5)	94.3972	89.7952	<b>93.3983</b> (3,4,5)	<b>99.0059</b> (3,9,5)	<b>99.1304</b> (3,4,5)	99.3193	97.7187	<b>99.2958</b> (3,4,5)
LM-Test Architecture	<b>92.2612</b> (3,5,5)	<b>92.0504</b> (3,10,5)	92.6710	86.2687	<b>92.7297</b> (3,3,5)	<b>99.0192</b> (3,5,5)	98.7908	99.0452	97.1497	<b>99.2417</b> (3,3,5)
RProp-Train	91.7322	92.3465	94.2465	89.8786	92.0171	98.8003	98.9374	99.3242	97.7675	99.2058
RProp -Test Architecture	90.5510	91.5441	92.5949	88.5802	91.5324	98.3773	98.3773	99.1112	<b>97.2680</b> (3,4,5)	99.1168

Table 38.: RSM method - Results of 100-MAPE

Surface roughness	100-MAPE				
	Ra	Rq	Rz	Rp	Rv
RSM	97.2563	97.0520	96.4014	89.6507	94.9921

Table 39.: RSM method - Results of R<sup>2</sup>

Surface roughness	R <sup>2</sup>				
	Ra	Rq	Rz	Rp	Rv
RSM	97.2563	97.0520	96.4014	89.6507	94.9921

Table 40.: ANN Results of 100-MAPE

ANN Optimiser	LM	LM	GD	GD/GDA	LM
Train	92.6582	93.3200	95.1854	90.1051	93.3983
Test	92.2612	92.2612	93.5771	89.4264	92.7297

Table 41.: ANN Results of R<sup>2</sup>

ANN Optimiser	LM	LM	GD	GD/GDA	LM
Train	99.0059	98.8806	99.4371	97.8093	99.2958
Test	99.0912	99.1304	99.3314	97.2687	99.2417